



**Analysis and control of convenient orbital configuration for  
formation flying missions**

**M. Sabatini, D. Izzo, G. Palmerini**

**16<sup>th</sup> AAS/AIAA Space Flight  
Mechanics Conference**

**Tampa, Florida**

**January 22-26, 2006**

**AAS Publications Office, P.O. Box 28130, San Diego, CA 92198**

# Analysis and control of convenient orbital configuration for formation flying missions

M. Sabatini<sup>✉</sup>, D. Izzo<sup>†</sup>, G.B. Palmerini<sup>‡</sup>

*Abstract*— The reduction of the amount of required orbital control is one of the drivers in formation flying missions design. This paper aims to contribute to this topic in two different ways: (i) by introducing a set of suitable reference orbits for which such an amount is quite low, and (ii) by investigating the performances offered by three different linear and nonlinear controllers. Results for this comparison are presented and discussed. Numerical simulations have been performed for the identified orbits as well as for the traditional circular projection formation.

## 1. INTRODUCTION

The interest in satellites flying in formation grows as the number of planned missions increases. One of the most urging questions concerns the possibility to achieve an orbital control effort as limited as possible. The answer is twofold: a first research area includes a deeper investigation on the formation dynamics, while a second addresses a proper choice of the control scheme. In this paper both aspects are analysed.

Regarding the study of dynamics, many authors have looked for invariant relative orbits: in this way the control effort needed to maintain the formation configuration would be minimum. Among others, Inalhan, Tillerson and How (Ref. 1) find the analytical form for the initial conditions of the classical Tshauer-Hempel equations; Kasdin and Koleman (Ref. 2) use the epicyclic orbital elements theory to derive bounded, periodic orbits in presence of various perturbations; Vaddi, Vadali, and Alfriend (Ref. 3) study a Hill-Clohessy-Wiltshire system modified to include second order terms; Schaub and Alfriend (Ref. 4) formulate the conditions for invariant  $J_2$  relative motion by means of the relations between mean orbit elements of the two satellites.

When the results based on simplified models are applied to an actual, fully perturbed, orbital environment, they often lose much of their interest. This is the main reason to pursue a numerical approach. In such a way, no approximations are needed on the dynamics analysed. As an example this path has been followed in (Ref. 5) using Genetic Algorithms (GA). One of the most interesting results obtained there is that, in a  $J_2$  perturbed environment, it is possible to identify particular reference orbits which

---

<sup>✉</sup> PhD candidate at the School of Aerospace Engineering, Università La Sapienza, Rome, Italy, [m.sabatini@email.it](mailto:m.sabatini@email.it)

<sup>†</sup> Advanced Concept Team, ESA ESTEC, Noordwijk, The Netherlands, [dario.izzo@esa.int](mailto:dario.izzo@esa.int)

<sup>‡</sup> Associate Professor, Aero/Astro Eng. Dept., Università La Sapienza, Rome, Italy, [giovanni.palmerini@uniroma1.it](mailto:giovanni.palmerini@uniroma1.it)

enable periodic relative trajectories. For circular orbits, they are characterized by an inclination which is either critical ( $63.4^\circ$ ) or belonging to a limited set around  $50^\circ$ . Section 2 will be devoted to a deeper discussion of this aspect.

Even for the periodic orbits found in this way, control actions are needed when other external forces, like air drag, higher harmonics of the geopotential, moon-sun attraction and solar pressure, are included in the dynamical models.

Therefore the attention will be focused on the choice of a proper control scheme. Concerning the selection of a suitable controller, McInnes (Ref. 6) and Palmerini (Ref. 7) study the possibility of applying Lyapunov methods to the satellites constellation. Queiroz, Kapila and Yan (Ref. 8) propose an adaptive nonlinear control based on the Lyapunov theory applied to a dynamical model including constant or slow-varying parameters and perturbations. Vaddi and Vadali (Ref. 9) apply a Lyapunov controller, a LQR controller and a period matching controller on a keplerian dynamical model; also Ulybishev (Ref. 10) analyses the possibility to use Linear Quadratic Regulators in the spacecraft control.

Section 3 presents a comparison among different proposed controllers. In detail, LQR controller is computed using classical Hill-Clohessy-Wiltshire model or more accurate schemes including oblateness or air drag effects. The aim is to lower the control effort by choosing a plant closer the actual dynamical environment. Next, the controller proposed in (Ref. 8) has been implemented and its performances have been evaluated neglecting part of the original hypothesis on the dynamics. Finally, a Lyapunov controller is proposed, computed on a fully perturbed model. The stability is therefore granted, while control cost can easily result quite high.

Control performances always depend on the trajectories to be tracked. Therefore, the controllers' simulations have been first carried out with respect to traditional circular projection formation. Moreover the identification of the reference state with the invariant relative orbits, supplied as a result of the dynamical analysis, is investigated in order to assess minimum consumption conditions.

## **2. CONVENIENT CONFIGURATIONS ANALYSIS**

In (Ref. 5) Genetic Algorithms have been used as a tool for the search of the invariant  $J_2$  configurations. The periodicity of relative motion does exist only if particular reference orbits are chosen. For a circular orbit, two inclinations allow to find invariant orbits: the critical inclination ( $63.4^\circ$ ) and another special inclination around  $50^\circ$ .

GA return, for each candidate configuration, the value of a fitness function which is an index of how much closed is the relative trajectory found. Figure 1 describes the behaviour of the fitness function for a circular orbit sweeping the whole range of inclinations.

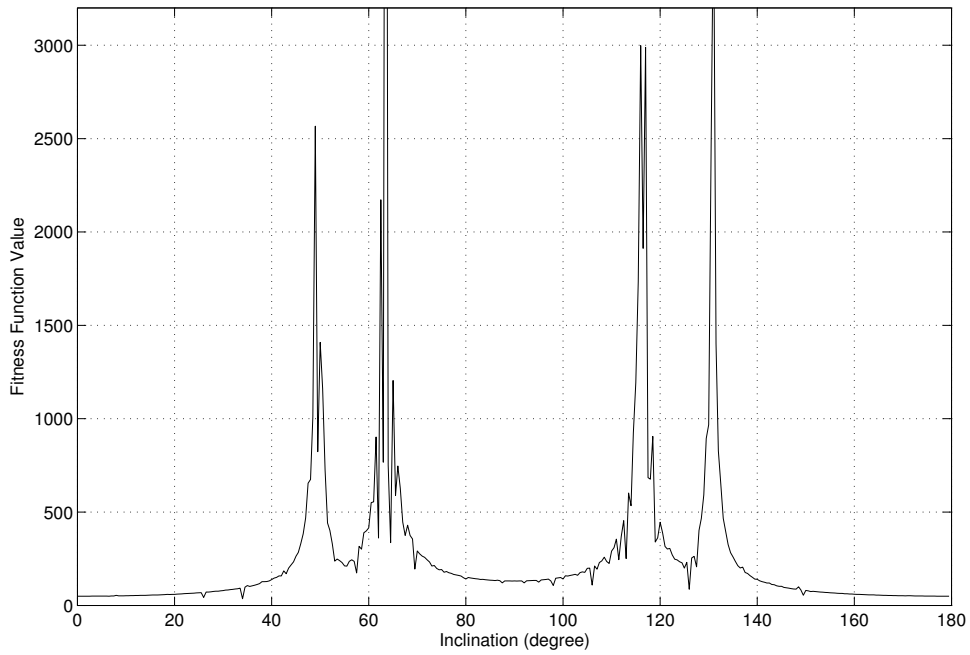


**Figure 1: Fitness function values for the whole range of inclination; circular case.**

While for the critical inclination an explanation has been provided in (Ref. 5), the  $50^\circ$  inclination is still unexplained. Figure 2 plots a zoom of the area under observation. A clear peak can be found at  $49^\circ$  inclination, but the entire range around  $49^\circ$  (say  $48^\circ$ - $50^\circ$ ) allows to find quasi-periodic relative orbits.

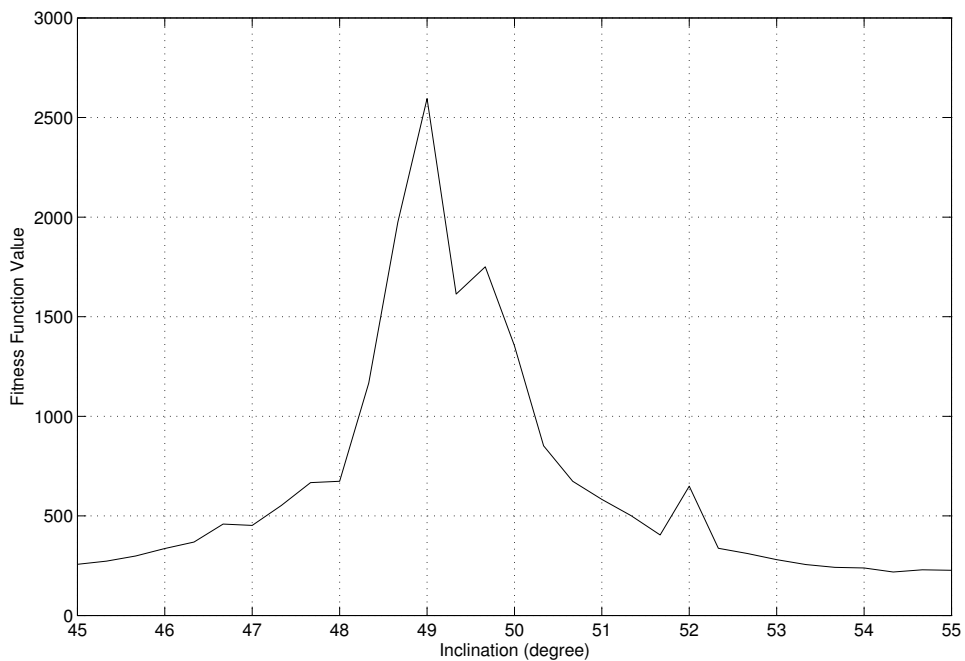


**Figure 2: Zoom of Figure 1**

In order to investigate the case, a linearized model for circular orbit, already proposed in (Ref. 11) has been used as a test. Eq. (1a) , (1b) and (1c) describe this model:

$$\dot{X} = AX \quad (1a)$$

where  $X = [x, y, z, \dot{x}, \dot{y}, \dot{z}]$  is the reference state in the Local Vertical Local Horizontal frame, and:

$$A = \begin{bmatrix} 0 & 0 & 0 & 1 & 0 & 0 \\ 0 & 0 & 0 & 0 & 1 & 0 \\ 0 & 0 & 0 & 0 & 0 & 1 \\ a & b & c & 0 & 2\omega_z & 0 \\ d & e & f & -2\omega_z & 0 & 2\omega_x \\ g & h & j & 0 & -2\omega_x & 0 \end{bmatrix} \quad (1b)$$

is the state matrix, where:

$$\begin{aligned} a &= -\left[-\omega_z^2 - 2n^2 - 4K(1 - 3\sin^2 i \sin^2 \theta)\right] \\ b &= -\left[-\dot{\omega}_z - 4K(\sin^2 i \sin 2\theta)\right] \\ c &= -(\omega_x \omega_z - 4K \sin 2i \sin \theta) \\ d &= \left[-\dot{\omega}_x - 4k \sin^2 i \sin 2\theta\right] \\ e &= -\left[n^2 - \omega_x^2 - \omega_z^2 - 4K\left(-\frac{1}{4} + \sin^2 i \left(\frac{7}{4} \sin^2 \theta - \frac{1}{2}\right)\right)\right] \\ f &= -\left[-\dot{\omega}_x + K(\sin 2i \cos \theta)\right] \\ g &= c \\ h &= -\left[\dot{\omega}_x + K(\sin 2i \cos \theta)\right] \\ j &= -\left[n^2 - \omega_x^2 - 4K\left(-\frac{3}{4} + \sin^2 i \left(\frac{5}{4} \sin^2 \theta + \frac{1}{2}\right)\right)\right] \end{aligned} \quad (1c)$$

where  $K = \frac{3J_2 \mu R_r^2}{2r^5}$  and  $i$ ,  $r$  and  $\theta$  have time-varying expressions;  $n$  is the mean motion and  $\omega_x$  and  $\omega_z$  the projections of the angular velocity. The results, reported in Figure 3 , are analogous to the those obtained for the nonlinear model. Thus the origins of the favourable inclination do not lay in the nonlinearities, but in a particular interaction between the first order  $J_2$  differential actions and the first order relative dynamics. The eccentricity also plays some role in finding these periodic configurations. In fact, the optimality of the  $50^\circ$  inclination decays as the eccentricity of the reference orbit grows (Figure 4).

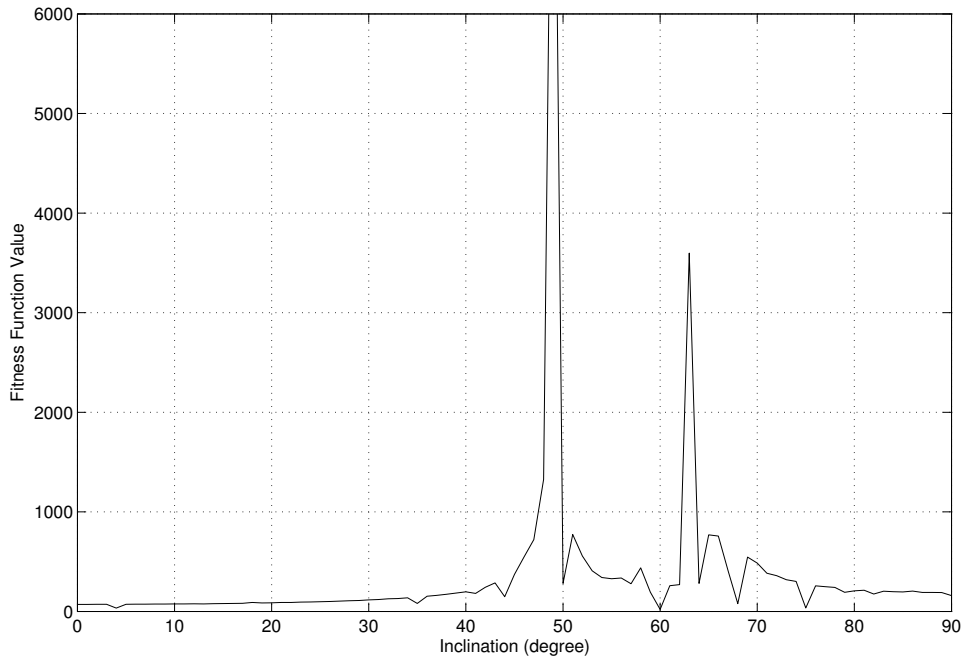


**Figure 3: Fitness Function Values for the linearized model.**

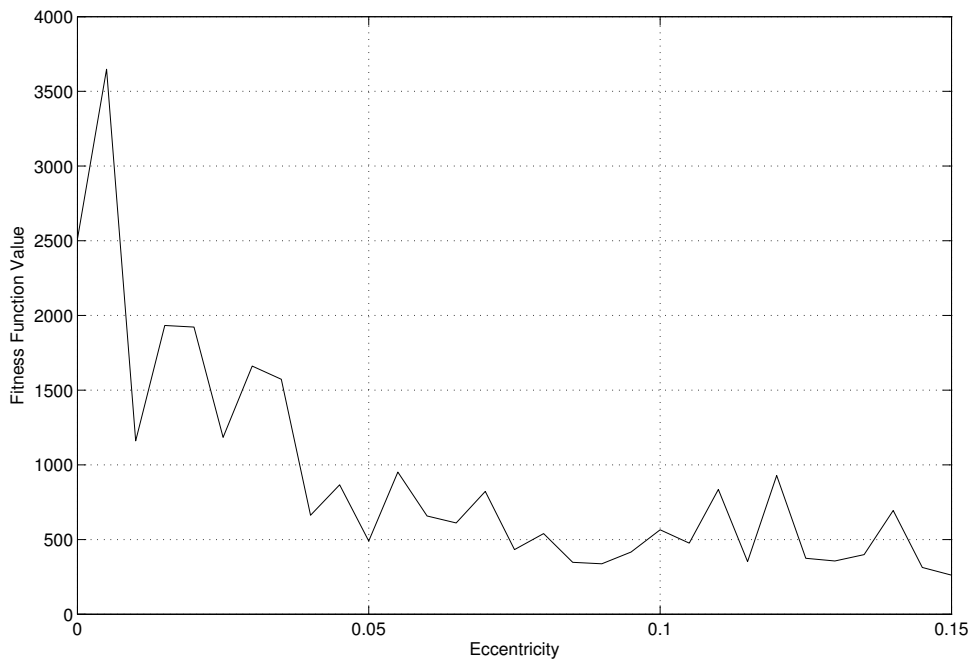


**Figure 4: Fitness Function Value at 50° for various eccentricities**

For generic non circular orbits, a complete mapping of the zones of interest will be necessary, such as the one provided in Figure 5. From this example, it is possible to affirm that a clear behaviour is available only for low eccentric orbits,  $e \in [0, 0.02]$ . For higher eccentricities, the levels of fitness function appear to have a higher mean, but

with a distribution which is difficult to describe, with two favourable bounded regions around  $50^\circ$  and  $65^\circ$  still present. Note that the plot presented in Figure 5, due to the stochastic nature of a GA approach, slightly changes when runs with different seeds and parameters are considered.

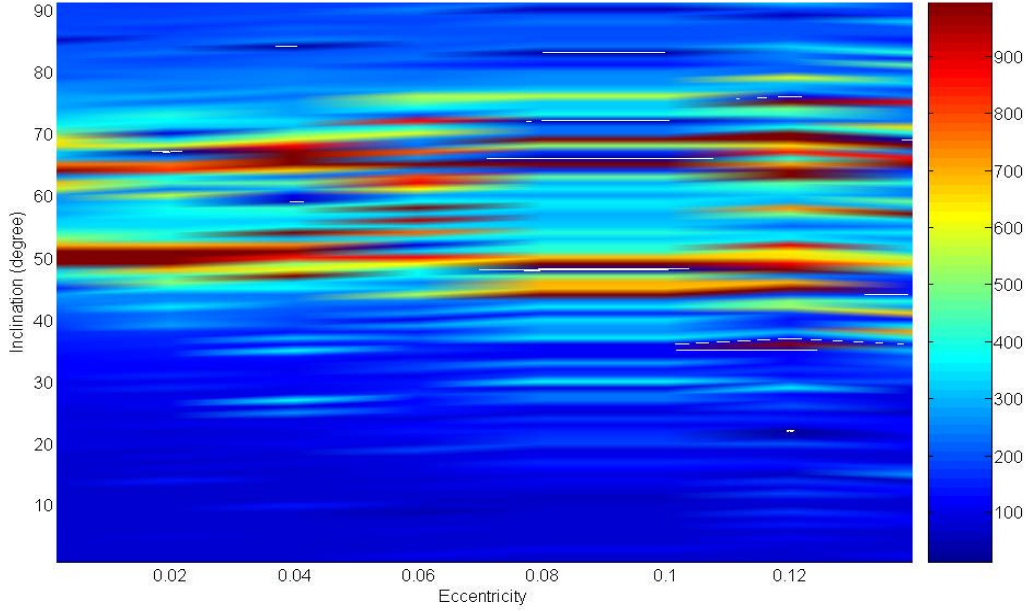


**Figure 5 Mapping of the preferable combinations of eccentricity and inclinations**

### 3. CONTROL SCHEMES ANALYSIS

Different strategies to maintain a desired formation configuration are possible. In the following three approaches will be considered: a Linear Quadratic, a nonlinear adaptive and a Lyapunov controller.

The computation of the  $\Delta V$  required by these three controllers has been performed by choosing as desired trajectory a classical circular projection configuration (Ref. 9) or an invariant relative orbit described in Section 2. Though the results are different according to which of the three control schemes is adopted, a better performance for the invariant orbit in terms of  $\Delta V$  saved is the common characteristic. This is the reason why these particular trajectories will be recalled in the following as *convenient*.

In Figure 6 and Figure 7 the two reference relative orbits are shown. The circular projection is a solution of the Hill-Clohessy-Wiltshire (HCW) equations, described by the equations:

$$\begin{cases} \bar{x}(t) = .5 \sin(nt) \\ \bar{y}(t) = \cos(nt) \\ \bar{z}(t) = \sin(nt) \\ \dot{\bar{x}}(t) = .5n \cos(nt) \\ \dot{\bar{y}}(t) = -n \sin(nt) \\ \dot{\bar{z}}(t) = n \cos(nt) \end{cases} \quad (2)$$

The *convenient* orbit is obtained as a propagation of the initial conditions supplied by the GA analysis. Of course, a necessary constraint is that the orbit of the formation can be described by a set of parameters corresponding to a “red zone” in the map in Figure 5 (the set  $a=6678\text{km}$ ,  $e=0$ ,  $i=49^\circ$  has been selected for this test). The initial relative state selected for this simulation: is given by:

$$\begin{aligned}
 \bar{x}_0 &= 8.205\text{E} - 2 \text{ km} \\
 \bar{y}_0 &= 0.816 \text{ km} \\
 \bar{z}_0 &= -3.056\text{E} - 3 \text{ km} \\
 \dot{\bar{x}}_0 &= -1.014\text{E} - 4 \text{ km/s} \\
 \dot{\bar{y}}_0 &= -1.912\text{E} - 4 \text{ km/s} \\
 \dot{\bar{z}}_0 &= 9.993\text{E} - 4 \text{ km/s}
 \end{aligned}
 \tag{3}$$

As a large formation would need a greater amount of  $\Delta V$  with respect to a small formation, two reference trajectories with a similar average separation between the spacecrafts (1.06 km for the circular projection case and 1.34 km for the *convenient* relative orbit) were chosen for the comparison.

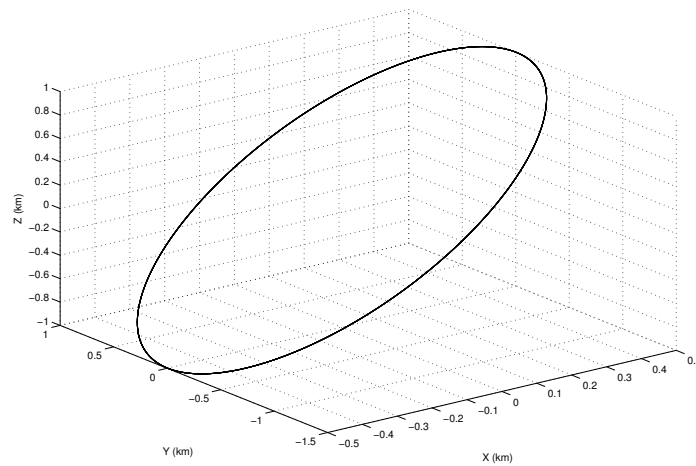


**Figure 6 Circular Projection relative orbit: 10 periods simulation**

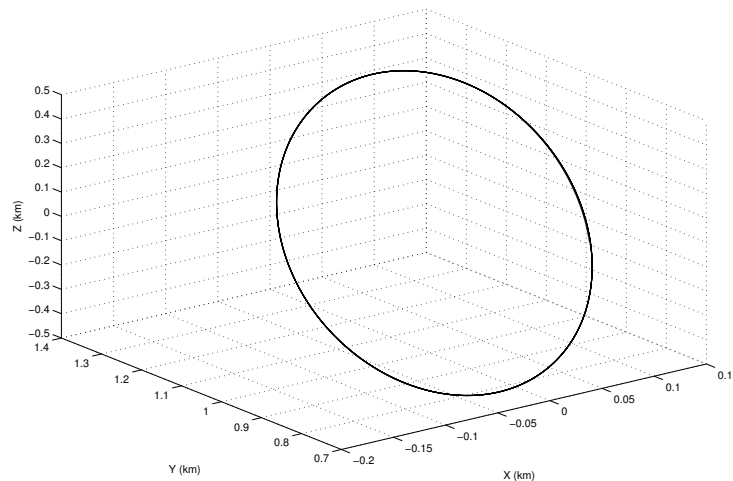


**Figure 7: Convenient relative orbit: 10 periods simulation**

### 3.1. LQR with improved dynamical plants

Linear Quadratic Regulator approach, (Ref. 12 and 13), is deemed to offer an optimal control strategy for the system

$$\dot{X} = AX + BU \quad (4)$$

with respect to a cost function based (i) on the closeness to a desired reference state (trajectory) all along the time interval of interest, and (ii) on the actuators' effort. These two different aspects are weighted by matrices  $Q$  and  $R$  in the classical formulation of the cost index:

$$J = \frac{1}{2} \int_{t_0}^{t_f} (X(t) - \bar{X}(t))Q(X(t) - \bar{X}(t))^T + URU^T dt \quad (5)$$

where  $\bar{X}$  is the reference state and  $X$  the state vector (relative position and velocity). The optimal solution is given by:

$$U(t) = R^{-1}(t)B^T(t)[G(t) - K(t)\bar{X}(t)] \quad (6)$$

where the vector  $G(t)$  (identically vanishing in the case of a system to be ideally kept at rest) is the solution of the differential equation

$$\dot{G}(t) = [K(t)B(t)R^{-1}(t)B^T(t) - A^T(t)]G(t) - Q(t)\bar{X}(t) \quad (7)$$

with the initial condition  $G(t_f) = \underline{0}$ , and  $K(t)$  is the solution of the Riccati equation

$$\dot{K}(t) = K(t)B(t)R^{-1}(t)B^T(t)K(t) - K(t)A(t) - A^T(t)K(t) - Q(t) \quad (8)$$

with the final condition  $K(t_f) = \underline{0}$ . Once matrices  $K(t)$  and  $G(t)$  have been evaluated, control actions following eq.(6) can be inserted in closed loop with a fully perturbed propagator representing the actual dynamics for the plant.

Three different linear models are considered. The first one is the classical Hill-Clohessy-Wiltshire (HCW) model, whose state matrix, obtained by imposing the hypothesis of circular keplerian motion and then linearizing, is:

$$A = \begin{bmatrix} 0 & 0 & 0 & 1 & 0 & 0 \\ 0 & 0 & 0 & 0 & 1 & 0 \\ 0 & 0 & 0 & 0 & 0 & 1 \\ 3n^2 & 0 & 0 & 0 & 2n & 0 \\ 0 & 0 & 0 & -2n & 0 & 0 \\ 0 & 0 & -n^2 & 0 & 0 & 0 \end{bmatrix} \quad (9)$$

The second one includes the  $J_2$  effects (called “ $J_2$ ” model in the following), which state matrix has been already reported in eq. (1b). Note that this state matrix is time-dependant, because inclination and radius are not considered as constant.

The third model takes into account the differential drag effects and has been proposed by Carter and Humi in (Ref. 14) (“CH” model in the following). The relevant equations, worked out for the application to LQR scheme result as:

$$\left\{ \begin{array}{l} \ddot{\tilde{x}} = 2\dot{\vartheta}\dot{\tilde{y}} + 3(1+4\alpha^2)\dot{\vartheta}^2\tilde{x} - \\ \quad - (\beta-\alpha)\left(-\dot{\vartheta}^2\tilde{y} + \dot{\vartheta}\dot{\tilde{x}} - 2\alpha\dot{\vartheta}^2\tilde{x} - 2\alpha\dot{\vartheta}^2 h^{-1/2}R_0^2 e^{-3\alpha\theta}\right) \\ \ddot{\tilde{y}} = -2\dot{\vartheta}\dot{\tilde{x}} + (\beta-\alpha)\left(-\dot{\vartheta}^2\tilde{x} - \dot{\vartheta}\dot{\tilde{y}} + 2\alpha\dot{\vartheta}^2\tilde{y} - \dot{\vartheta}^2 h^{-1/2}R_0^2 e^{-3\alpha\theta}\right) \\ \ddot{\tilde{z}} = -\dot{\vartheta}^2\tilde{z} - (\beta-\alpha)\left(\dot{\vartheta}\dot{\tilde{z}} - 2\alpha\dot{\vartheta}^2\tilde{z}\right) \end{array} \right. \quad (10)$$

Some additional manipulation (Ref. 15) is necessary, as these equations are not yet in the desired form  $\dot{X} = A(t)X$  because of the non-dimensional variables  $[\tilde{x}, \tilde{y}, \tilde{z}]$  used.

Assuming that satellites have same mass and structural properties, which minimizes the differential drag effects, the simulation of the controlled system is performed with the circular projection and with the *convenient* reference relative trajectory. The resulting  $\Delta V$  required by the three different LQR controllers are plotted in Figure 8 and Figure 9.

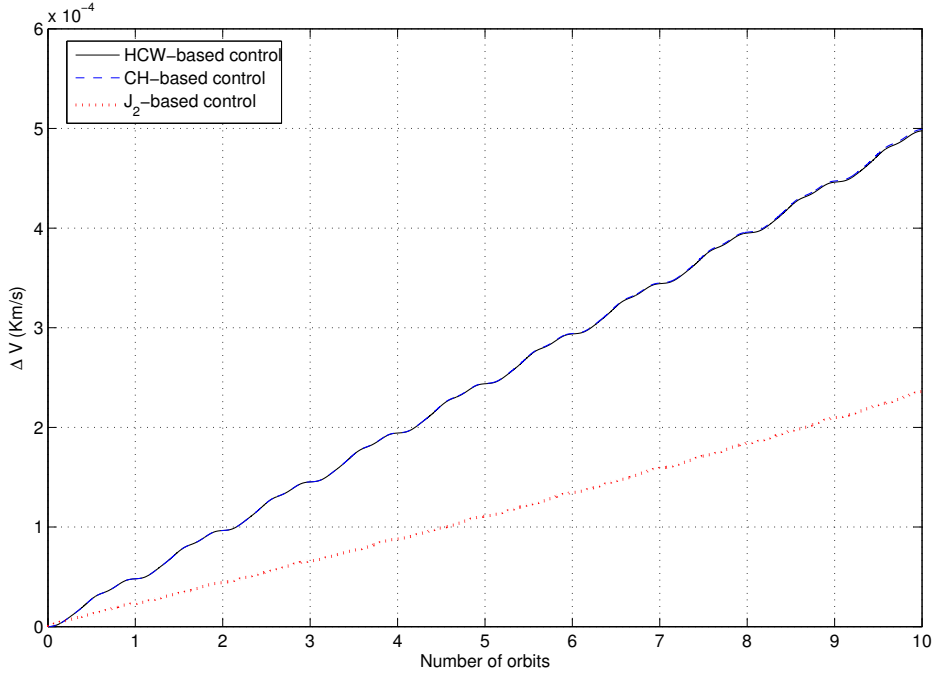


**Figure 8: LQR performances for the circular projection reference orbit**

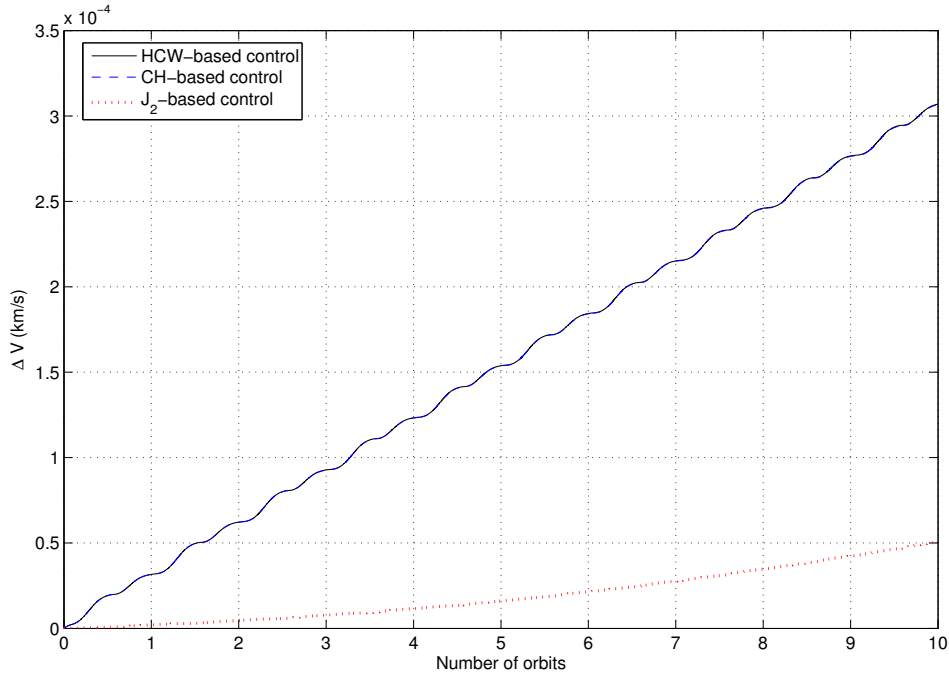


**Figure 9 LQR performances for the convenient reference orbit**

Such analysis provides three main results. First, a proper choice of the linear dynamical plant represented by matrix  $A(t)$  can greatly influence final results. Second, the *convenient* orbit allows to save a great amount of  $\Delta V$ , as table 1 shows. Third, to consider drag effects in the dynamic models used to solve eq. (7) and eq. (8) is a useless complication for a formation of equal spacecraft at the altitude considered. In fact, CH curves in Figure 8 and Figure 9 are overlapped to the HCW curves. Instead to include  $J_2$  perturbation proves to be a relevant improvement.

	HCW-based controller	CH-based controller	J <sub>2</sub> -based controller
$\Delta V$ :circular projection case	4.98e-4 km/s <sup>2</sup>	4.98e-4 km/s <sup>2</sup>	2.37e-4 km/s <sup>2</sup>
$\Delta V$ : <i>convenient</i> case	3.07e-4 km/s <sup>2</sup>	3.07e-4 km/s <sup>2</sup>	0.51e-4 km/s <sup>2</sup>

**Table 1  $\Delta V$  required for a 10 orbits trajectory tracking**

However, CH model is of interest in other situations (see also Ref. 15). In fact, when the two spacecraft present a different area to mass ratio the differential drag effects are much more important, and using a model which includes them is a significant improvement with respect to simple HCW model.

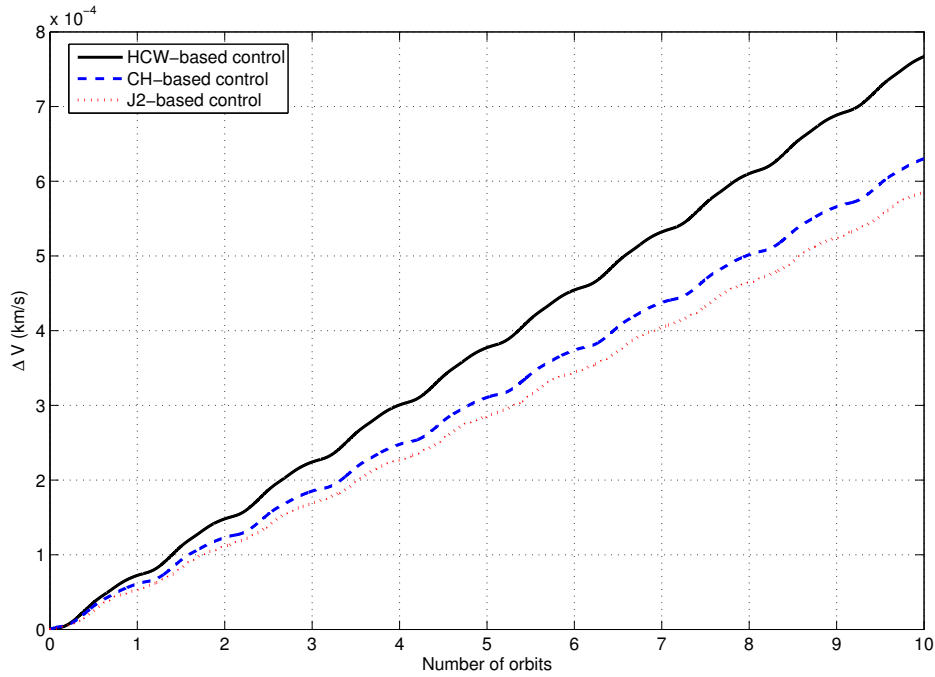


**Figure 10 LQR performances for the convenient reference orbit: strong differential drag case**

Figure 10 reports the case of a follower with a ballistic parameter which is 70% of the leader's one. Control effort computed by  $J_2$  model is still advantageous, but the usefulness of CH with respect to HCW begins to appear. Differences between the two perturbed dynamics vary with the ratio of the two cross sections  $\frac{A_{FOLLOWER}}{A_{LEADER}}$ .

Figure 11 shows that increasing this ratio, the control effort grows in both cases, because of the augmented perturbing action of drag; but the CH-based control is able to counteract this effect better than the  $J_2$ -based model, so that there exist values of  $\frac{A_{FOLLOWER}}{A_{LEADER}}$  which make CH-based control preferable.

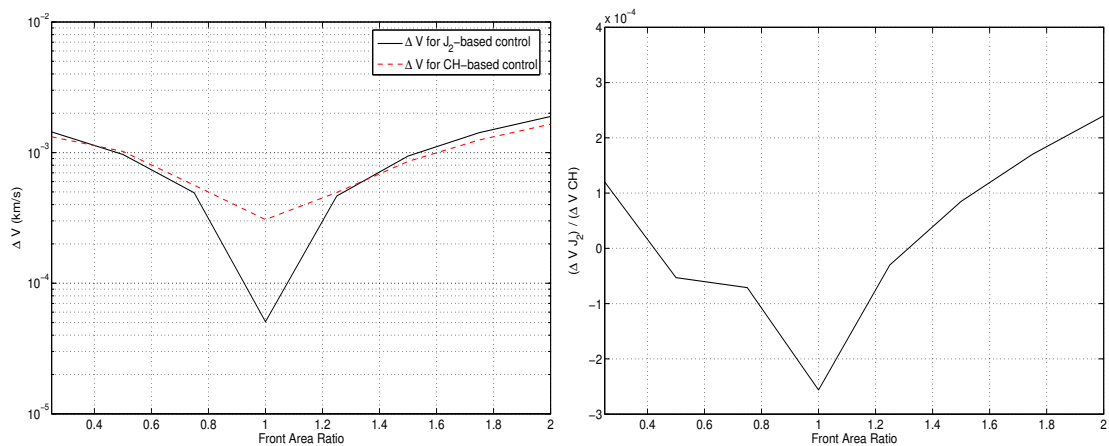


**Figure 11 J<sub>2</sub>-based and CH-based LQR performances for different satellites front area ratios**

Note that the symmetry of the  $\Delta V$  curves with respect to the unity ratio is only apparent, as (i) the control is applied on the follower satellites alone and not on both spacecraft, and (ii) the front area of the leader is fixed, thus the cases  $\frac{A_{FOLLOWER}}{A_{LEADER}} = x$  and  $\frac{A_{FOLLOWER}}{A_{LEADER}} = \frac{1}{x}$  do not describe two equivalent situations, being the total area exposed to atmosphere different, and so the drag effect.

### 3.2. Adaptive Nonlinear Control

In (Ref. 8) Queiroz, Kapila and Yan propose a Lyapunov-based, nonlinear, adaptive control law that guarantees global asymptotic convergence of the position tracking error in the presence of unknown, constant or slow-varying spacecraft masses, disturbances forces and gravity forces.

Dynamics is given by:

$$m_f \ddot{q} + C(\omega)\dot{q} + N(q, \omega, R, u_l) + F_d = u_f \quad (11)$$

where  $q=[x,y,z]$  is the state vector,  $\omega$  the angular velocity,  $C(\omega)$  and  $N(q, \omega, R, u_l)$  two matrices representing the formation keplerian dynamics,  $F_d$  the approximated perturbations (constant or slow-varying) and  $u_f$  the follower control actions.

The control law proposed is given by:

$$u_f = W\hat{\theta} + Kr \quad (12)$$

where  $W$  is a matrix depending on the state, on the errors and on the desired trajectory;  $\hat{\theta}$  is a vector of the parameters (basically spacecrafts masses and disturbances);  $K$  is a gain matrix and  $r$  is representative of the error, being:

$$r = \dot{e}(t) + \Lambda e(t) \quad (13)$$

with  $e$  the error vector and  $\Lambda$  a constant matrix. The stability of this controller is proved in (Ref. 8) with respect to the model in eq. (11) which could not represent the actual environment conditions, as the one provided by the complete propagator used. However, the adaptive nonlinear control has proved to fit this case as well. Figure 12 shows the comparison in terms of  $\Delta V$  for the two reference relative trajectories.

In this case, as for LQR case, it is clear how keeping the formation on the *convenient* trajectory is much easier, resulting in a lower  $\Delta V$ .

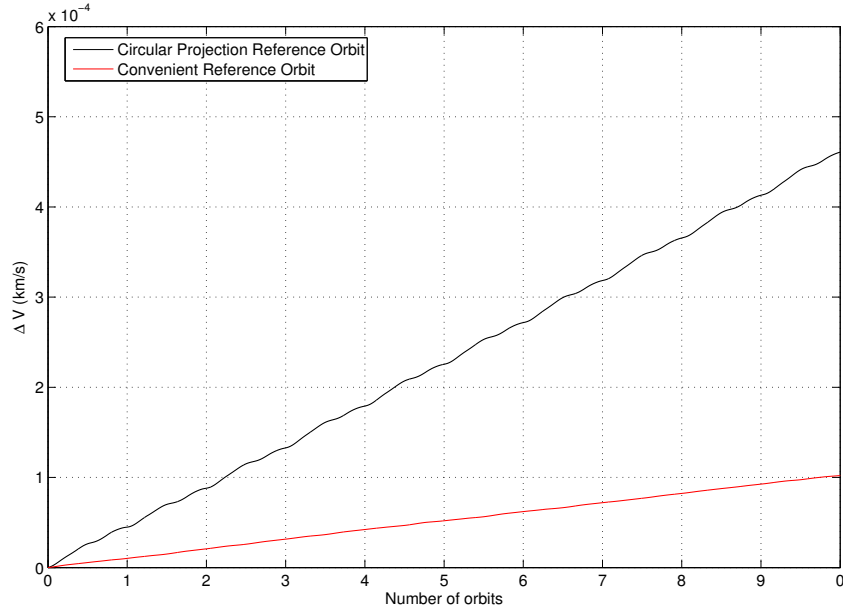


**Figure 12 Nonlinear adaptive controller performances for the two reference orbits**

### 3.3. Lyapunov controller

The so-called Lyapunov second method provides stable controller for nonlinear dynamical models by introducing the potential function  $V$  which respect the conditions:

$$\begin{aligned}
 V(e) &> 0 \text{ for all } e \neq 0 \\
 \dot{V}(e) &< 0 \text{ for all } e \neq 0 \\
 V(e) &\rightarrow \infty \text{ with } \|e\| \rightarrow \infty \\
 V(0) &= 0
 \end{aligned} \tag{14}$$

In eq. (14),  $e = X - \bar{X}$ , being  $X = [x, y, z]^T$  the three state variables describing the projection of the relative distance on the three axes, and  $\bar{X} = [\bar{x}, \bar{y}, \bar{z}]^T$  the corresponding components of the reference relative trajectory.

Because of the first of eq. (14), the potential function  $V$  is chosen as

$$V = \alpha e^T e + \beta \dot{e}^T \dot{e} \tag{15}$$

with  $\alpha, \beta$  positive scalar. Deriving with respect to time:

$$\frac{dV}{dt} = 2\alpha \dot{e}^T e + 2\beta \dot{e}^T \ddot{e} \tag{16}$$

In order to satisfy the second of eq. (14), it is possible impose:  $\frac{dV}{dt} = -2\gamma \dot{e}^T \dot{e} < 0$  with  $\gamma > 0$ .

In eq. (16):

$$\ddot{e} = \ddot{X} - \ddot{\bar{X}} = Din(X, \dot{X}, par) + U - \ddot{\bar{X}} \quad (17)$$

where  $Din(X, \dot{X}, par)$  are the dynamics to be controlled. In the case of a fully perturbed formation flying:

$$Din(X, \dot{X}, par) = -2\bar{\omega} \times \dot{\bar{X}} - \bar{\omega} \times (\bar{\omega} \times \bar{X}) - \dot{\bar{\omega}} \times \bar{X} + \nabla \bar{F} \quad (18)$$

where  $\nabla \bar{F}$  represents the gradient of all the forces acting on the satellites. In the present paper the propagator included other than Keplerian gravitational attraction, 23 zonal and 8 tesseral harmonics of the geopotential, the air drag modelled according to Jacchia's atmosphere model, the moon and sun attraction and the solar pressure.

Substituting in eq. (16), it is possible to write:

$$2\dot{e}^T \left[ \alpha \cdot e + \beta \cdot Din(X, \dot{X}, par) + \beta U - \beta \ddot{\bar{X}} \right] = -2\gamma \cdot \dot{e}^T \dot{e} \quad (19)$$

It is now easy to write the expression for the control actions:

$$U = -\frac{\alpha}{\beta} e - Din(X, \dot{X}, par) + \ddot{\bar{X}} - \frac{\gamma}{\beta} \dot{e} = -K_1 e - Din(X, \dot{X}, par) + \ddot{\bar{X}} - K_2 \dot{e} \quad (20)$$

where  $K_1$  is an index of the ratio of the magnitude of the variables  $e$  and  $\dot{e}$ , while  $K_2$  is related to the control amplitude, being the derivative of  $V$  proportional to  $\gamma$ .

$\Delta V$  plotted in Figure 13 have been obtained for the circular projection and for the *convenient* reference trajectory performing as before the simulation and using for the parameters the values  $K_1=10^{-6}$ ,  $K_2=10$ . Again, the *convenient* reference orbit configuration outperforms the traditional circular projection one.

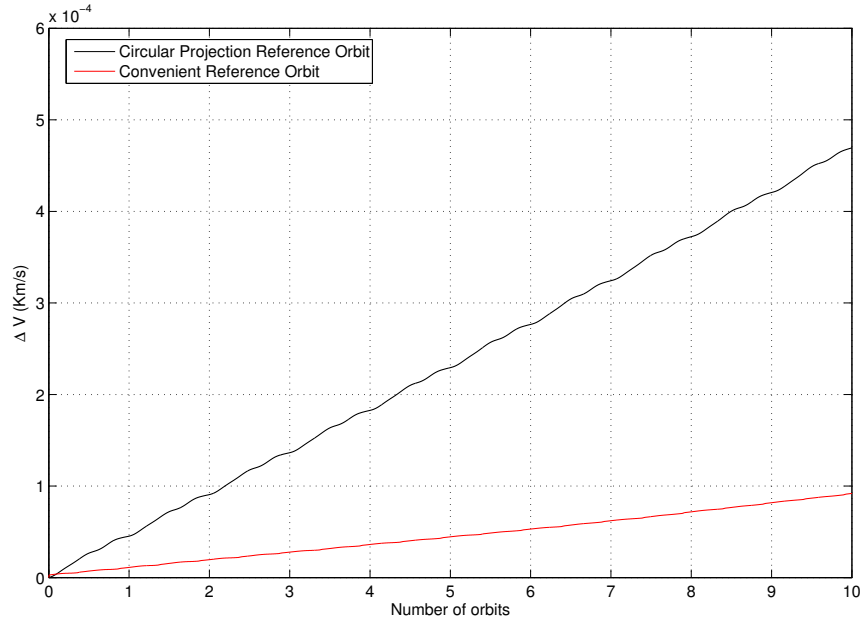


Figure 13 Lyapunov controller performances for the two reference orbits

### 3.4. Controllers Comparison

Results of the three control schemes for the *convenient* case are plotted together in Figure 14, while Figure 15 shows the errors on the relative position. Such a comparison depends of course on the choice of the gain parameters and matrices and it cannot therefore be considered as a final assessment of the controllers' cost. However it can be stated that a LQR controller properly implemented (meaning: with the right choice of linear dynamical plant) grants better performances with respect to a nonlinear controller for a wide range of situations, in terms of  $\Delta V$  required: on the other hand, the errors on the desired trajectory are very small, but not necessarily converging. In fact there is no certainty of stability when applying a LQR control law to a nonlinear propagator. Instead, a Lyapunov controller grants stability of the system, though not reaching optimality in terms of  $\Delta V$  required, which is usually much higher than the LQR case. The nonlinear adaptive control is again stable, but with respect to the simplified dynamics it has been computed on and not to the fully perturbed model. This means that the stability, though appearing confirmed in these cases, is not theoretically proved. In all tests performed, choosing a *convenient* reference orbit resulted in a huge advantage and could be a critical driver in a study for a formation mission feasibility.

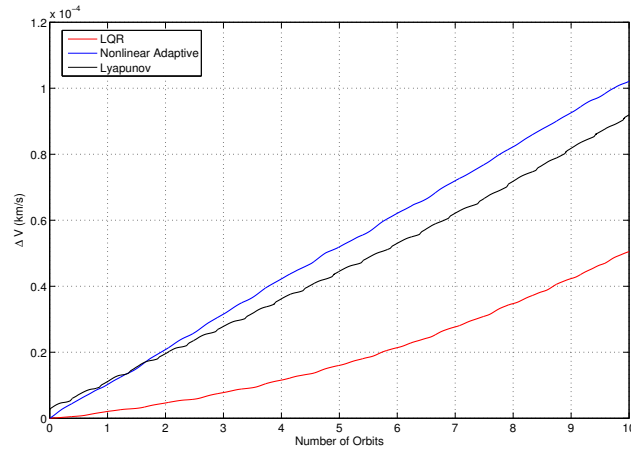


Figure 14 Comparison in terms of  $\Delta V$  required

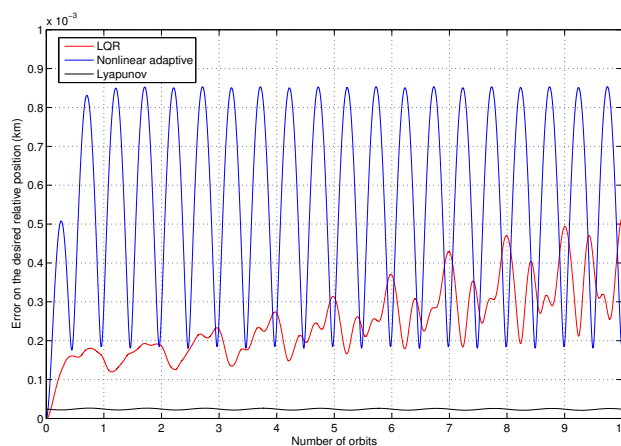


Figure 15 Comparison in terms of error on the relative position

#### 4. CONCLUSIONS

Orbital control performances in formation flying missions depend on the targeted configuration as well as the control strategies adopted. This paper presented some investigation on low-altitude formations, addressing both aspects.

Concerning the configuration, the possibility to make use of relative trajectories, numerically identified by genetic algorithms, has been deeply analysed. If  $J_2$  effect is taken into account, there is a limited range of eccentricity and inclination where these trajectories are periodic. Interestingly, controlling along these special relative trajectories results in a great  $\Delta V$  saving with respect to other configuration like the classical circular projection.

As far as it concerns the control strategies, three different approaches have been compared in a fully perturbed environment. The LQR outperforms the other schemes regarding the control effort, but, though very precise, it does not ensure its stability: in fact, the errors slowly grow with time. LQR's gain matrices have been computed with different dynamics including  $J_2$  and drag effects, showing that best results can be accomplished by selecting a model as close as possible to the actual environment. A nonlinear adaptive controller found in literature presents higher errors and  $\Delta V$ , but has a wider stability field; finally, a controller directly derived by Lyapunov second method also offers very small and bounded errors: its stability is theoretically proved, but the  $\Delta V$  is greater than LQR's one.

#### Acknowledgments:

This work has been partially funded by the Advanced Concepts Team of the European Space Agency under the Contract 18141/04/NL/MV, Project Ariadna AO04/4104

#### REFERENCES

- [1] Inalhan G., Tillerson M., How J. P., "Relative dynamics and control of spacecraft formations in eccentric orbits", *Journal of Guidance, Control and Dynamics*, Vol. 25, No. 1, 2002, pp. 48-59.
- [2] Kasdin N. J., Koleman E., Bounded, "Periodic Relative Motion using Canonical Epicyclic Orbital Elements", Paper AAS 05-186, 15<sup>th</sup> AAS/AIAA Space Flight Mechanics Meeting, Copper Mountain, Colorado, 2005
- [3] Vaddi S. S., Vadali S.R., and Alfriend K.T., "Formation Flying: Accommodating Nonlinearities and eccentricity Perturbations", *Journal of Guidance, Control, and Dynamics*, Vol. 26, No. 2, March-April 2003, pp. 214-223.

- [4] Schaub H., Alfriend K.T., “ $J_2$  invariant relative orbits for spacecraft formations,” *Celestial Mechanics and Dynamical Astronomy*, Vol. 79, 2001, pp. 77-95.
- [5] M. Sabatini, R. Bevilacqua, M. Pantaleoni, D. Izzo , “Periodic relative motion of formation flying satellites”, AAS/AIAA 06-206, Space Flight Mechanics Meeting Tampa, Florida, January 22-26
- [6] C.R. McInnes, “Autonomous Proximity Manoeuvring Using Artificial potential Function”, *ESA Journal* 1993, v.17, pp159-169
- [7] G.B. Palmerini, “Coordinated Orbital Control For Satellite Constellations and Formations”, in (H. Ziomeck et al., eds) “Dynamics of Natural and Artificial Celestial Bodies”, Kluwer Academic Pub., 2001, pp. 415-424
- [8] M. S. de Queiroz, V. Kapila, and Quiguo Yan, “Adaptative Nonlinear Control of Multiple Spacecraft Formation Flying”, *Journal of Guidance, Control, and Dynamics*, Vol. 23, No. 3, May-June 2000.
- [9] S.S. Vaddi and S.R. Vadali, “Linear and Nonlinear Control Laws for Formation Flying”, 13<sup>th</sup> AAS/AIAA Space Flight Mechanics Meeting, 9-13 February 2003.
- [10] Y. Ulybishev, “Long-Term Formation Keeping of Satellite Constellation using Linear-Quadratic Controller”, *Journal of Guidance, Control and Dynamics* vol.21, no.1, Jan-Feb98, pp.109-115
- [11] Izzo D., Sabatini M., Valente C., “A new linear model describing formation flying dynamics under  $J_2$  effects”, *Proceedings of 17th AIDAA national congress Rome, ITA*, 15-19 September 2003, Vol.1, pp.493-500.
- [12] A.E. Bryson, “Control of Spacecraft and Aircraft”, Princeton University Press, Princeton (NJ, USA), 1994.
- [13] C. Bruni and G. Di Pillo, “Metodi Variazionali per il Controllo Ottimo”, Masson-ESA, Milano (Italy), 1993.
- [14] T. Carter and M. Humi, “The Clohessy-Wiltshire Equations can be Modified to Include Quadratic Drag”, Paper AAS 03-240, 13<sup>th</sup> AAS/AIAA Space Flight Mechanics Meeting, Ponce (Puerto Rico), Febr. 2003.
- [15] M. Sabatini, G.B. Palmerini, “Control Effort Evaluation for Low-Altitude Formation Flying”, 2006 IEEE Aerospace Conference 4-11 March 2006